DISTURBANCE OBSERVER-BASED PRACTICAL CONTROL OF SHAKING TABLES WITH NONLINEAR SPECIMEN

Makoto Iwasaki * **Kensuke Ito** *
Motohiro Kawafuku * **Hiromu Hirai** *
Yoshihiro Dozono ** **Katsuhiko Kurosaki** ***

* *Nagoya Institute of Technology, Nagoya, Japan*
** *Mechanical Engineering Research Laboratory, Hitachi, Ltd., Ibaraki, Japan*
*** *Hitachi Industries Co., Ltd., Ibaraki, Japan*

Abstract: This paper presents a practical control methodology of shaking tables for earthquake simulators. Reaction force generated by a nonlinear specimen on the shaking table generally deteriorates the motion performance of the table, resulting in the lower control accuracy of the seismic tests. In order to provide the precise table motion, therefore, a disturbance observer-based control approach is adopted, where the unknown disturbances in the table can be compensated in real time manner. The proposed compensation algorithm has been verified by experiments using an actual shaking table system.

Keywords: disturbance observers, earthquake simulators, seismic tests, shaking tables, reaction force compensation, nonlinear structure

1. INTRODUCTION

Shaking table system is one of indispensable components in a variety of earthquake simulators, where the desired table motion performance in acceleration and/or displacement should be exactly reproduced to perform seismic tests(Queval and Sollogoub, 1997), (Nowak *et al.*, 2000), and (Okuda *et al.*, 2001). The table system generally consists of electro-hydraulic actuators, sensors, a table, and a target specimen. Analytical studies on dynamics of the system and/or typical requirements in the simulators have been already discussed in previous literatures(Clark, 1992) and (Nowak *et al.*, 2000).

A deterioration in the table motion performance due to nonlinear behaviors of specimen should be inherent problems: the table motion is affected by the reaction force generated by the specimen as well as by the original driving force of the actuators, resulting in the lower control accuracy of the seismic test such as a damage process during excitation(Dozono *et al.*, 2004). In order to compensate for the effects and to achieve the precise table motion, various approaches have been proposed, e.g., using adaptive control and/or MCS techniques (Stoten and Gomez, 1998) and (Gomez and Stoten, 2000), and a real-time compensation (Dozono *et al.*, 2004).

This paper proposes a novel control methodology for the shaking tables using a disturbance observer(Ohnishi *et al.*, 1996), which is one of promising approaches to compensate for the nonlinearities of specimen in real time manner. The proposed control is verified by experiments using an actual uni-axial shaking table, especially paying attention to the reproducibility of frequency power spectrum in the desired table acceleration.

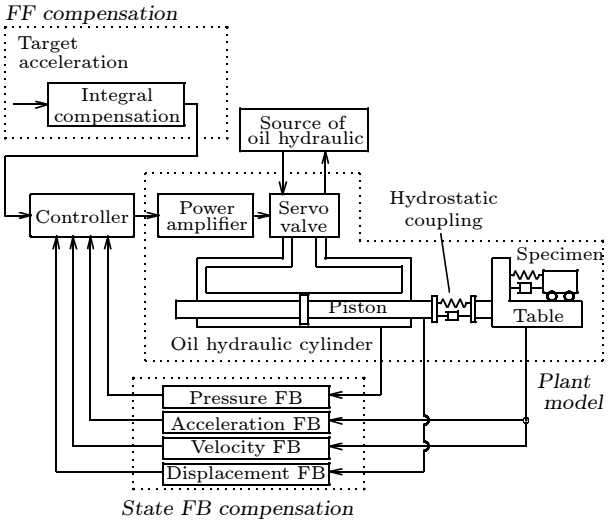

Fig. 1. System configuration of uni-axial shaking table.

2. SYSTEM CONFIGURATION OF SHAKING TABLE

2.1 System Configuration

Fig.1 shows a system configuration of uni-axial shaking table for the seismic tests. The mechanism as a plant system is composed of the shaking table with a specimen, coupled onto an oil hydraulic cylinder by a hydrostatic coupling. The specimen is constructed by weights and beams, where the natural frequency of the mechanical resonance is variable by adjusting the length of beams, simulating the nonlinear behavior in specimen. The cylinder as an actuator is driven by a power amplifier through a servo valve, where the table is horizontally shaken by applying the target acceleration reference. In actual seismic tests, the actuator is conventionally controlled by the state feedback compensation, using measured displacement, velocity, acceleration, and pressure.

The following are the mathematical expressions for the mechanical plant system.

Servo valve The servo valve can be characterized by a second-order lag system as follows, where the flow rate decreases due to the oil leakages proportional to the pressure:

$$Q_m = \frac{K_{sv}\omega_{sv}^2}{s^2 + 2\zeta\omega_{sv}s + \omega_{sv}^2} V_e - C_{al}P_m. \qquad (1)$$

Here, Q_m: flow rate of servo valve, V_e: output of controller, P_m: differential pressure of actuator in cylinder, K_{sv}: gain of power amplifier, ω_{sv} and ζ: natural frequency and damping coefficient of second-order model for servo valve, and C_{al}: oil leakage coefficient in cylinder.

Oil hydraulic cylinder The flow rate of oil in the cylinder is in proportion to the compression of oil and the variation of internal pressure in the cylinder and piping:

$$Q_m = A_a\, sY_p + K_a\, sP_m, \qquad (2)$$

where Y_p: displacement of piston, A_a: piston area, and K_a: stiffness of piston.

Kinetic equation of piston and table with specimen The table is driven by the shaking force of actuator through the hydrostatic coupling, where the mechanical motion can be expressed using the following kinetic equations:

$$M_a\, s^2Y_p = A_aP_m - N_t - C_{af}\, sY_p, \qquad (3)$$

$$N_t = C_j(sY_p - sY_t) + K_j(Y_p - Y_t), \qquad (4)$$

$$M_t\, s^2Y_t = N_t - D, \qquad (5)$$

where Y_t: displacement of table, D: reaction force of specimen, M_t: mass of table, M_a: effective mass of piston, C_{af}: viscosity coefficient of piston, C_j: viscosity coefficient of coupling, K_j: stiffness of coupling, and N_t: driving force of piston.

The specimen, on the other hand, is composed of a one-degree-of-freedom system as follows, where the reaction force of specimen to table can be characterized as the following disturbance D:

$$M_b\, s^2Y_z = D, \qquad (6)$$

$$D = C_b(sY_t - sY_z) + K_b(Y_t - Y_z). \qquad (7)$$

Here, Y_z: displacement of specimen, C_b: viscosity coefficient of specimen, K_b: stiffness of specimen, and M_b: mass of specimen.

Based on the mathematical models above, Fig.2 shows a whole block diagram of the shaking table, where the actual mechanical parameters are indicated in Table 1.

Table 1. Specifications of shaking table parameters.

K_{sv}	4.01×10^{-4} [Vm^3/s]	W_{sv}	3.43×10^{2} [rad/s]
ζ	1.42	C_{al}	9.37×10^{-12} [m^{3}Pa/s]
A_a	6.18×10^{-3} [m^2]	K_a	1.42×10^{-13} [m^3/Pa]
M_t	2.70×10^{3} [kg]	M_a	1.90×10^{2} [kg]
C_{af}	3.91×10^{3} [Ns/m]	C_j	5.83×10^{4} [Ns/m]
K_j	4.13×10^{8} [N/m]	M_{b1}	0.59×10^{3} [kg]
M_{b2}	0.59×10^{3} [kg]	M_{b3}	0.59×10^{3}
C_{b1}	28.61 [Ns/m]	C_{b2}	48.71 [Ns/m]
C_{b3}	97.86 [Ns/m]	K_{b1}	3.47×10^{5} [N/m]
K_{b2}	1.00×10^{8} [N/m]	K_{b3}	4.06×10^{8} [N/m]

2.2 Conventional table control using state feedback

The actuator for shaking table is generally driven in a state feedback control manner using the measured pressure and displacement of piston, and the measured velocity and acceleration of table, as shown in Fig.1, where the feedback gains can be designed by a pole-assignment technique considering the system stability and the disturbance

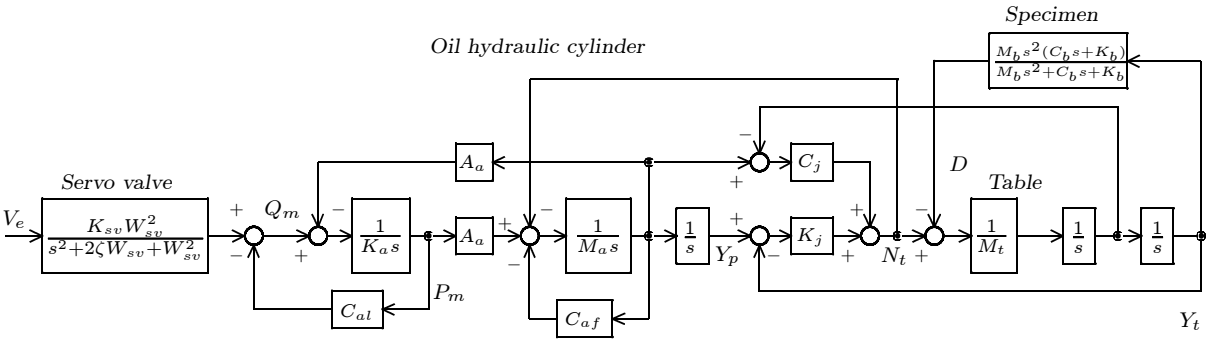

Fig. 2. Block diagram for mathematical model of shaking-table.

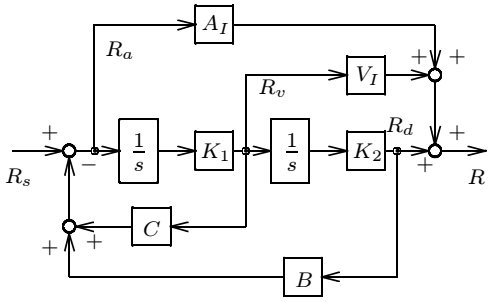

Fig. 3. Integral compensation for displacement reference.

suppression. The table displacement reference, in addition, is generated based on the acceleration profile through an "integral compensation" in a feedforward manner, which is directly specified as the seismic waveform.

Feedforward control by integral compensation The feedforward compensator generates the table displacement reference R as indicated in Fig.3, by means of the following integral compensation using the desired acceleration profile R_s:

$$R = A_I R_a + V_I R_v + R_d, \tag{8}$$

where R_a, R_v, and R_d: internal variables in the integral compensator, A_I and A_V: gains. These internal variables correspond to the acceleration, the velocity, and the displacement, leading the following relations for R_s by the second order filters:

$$R_a = A_I \frac{s^2 + (C - K_1 C)s + K_2 B - K_1 K_2 B}{s^2 + Cs + K_2 B} R_s,$$
$$R_v = V_I \frac{K_1 s}{s^2 + Cs + K_2 B} R_s,$$
$$R_d = \frac{K_1 K_2}{s^2 + K_1 Cs + K_1 K_2 B} R_s,$$

where B and C: stiffness and damping coefficients of second order filter, K_1 and K_2: coefficients for velocity and displacement.

State feedback control The control output V_e is calculated by the following feedback control law for the displacement reference R:

Table 2. Parameters in state feedback controller.

K_{ad}	1.60×10^{2} [V/m]	K_{ta}	8.16×10^{-1} [Vs^2/m]
K_{pr}	4.08×10^{-7} [V/Pa]	F_{tv}	-1.00×10^{-1}
F_{ta}	3.50×10^{-2}	F_{pr}	9.00×10^{-2}
F_p	4.00	τ_{int}	3.18×10^{-2} [s]
K_1	20	K_2	10
C	0.12	B	0.25
A_I	0.80×10^{-2}	V_I	0.12
T_s	0.2×10^{-3} [s]		

$$\begin{aligned} V_e &= kR - k_1 Y_p - k_2 Y_{tv} - k_3 Y_{ta} - k_4 P_m \\ &= E - K_{pr} F_{pr} P_m, \end{aligned} \tag{9}$$

$$\begin{aligned} E &= F_p K_{ad}(R - Y_p) \\ &\quad - F_{tv} \frac{K_{ta}}{1 + \tau_{int} s} Y_{ta} - F_{ta} K_{ta} Y_{ta}, \end{aligned} \tag{10}$$

where Y_{ta}: table acceleration, Y_{tv}: table velocity, F_p: proportional gain, K_{ad}, K_{ta}, and K_{pr}: voltage conversion gains for displacement, acceleration, and pressure, F_{tv}, F_{ta}, and F_{pr}: feedback gains for table velocity, table acceleration, and cylinder pressure, and τ_{int}: integration time constant.

Table 2 indicates parameters of the state feedback control with the reference integral compensation, where the whole control processing is implemented in the digital control manner with a sampling period of T_s. Fig.4 shows a typical acceleration reference waveform, where the reference includes the trapezoidal-shape frequency power spectrum with the target seismic frequency bandwidth up to 20 Hz. In the following experimental verifications, the reproducibility of the desired power spectrum is especially evaluated.

Fig.5 indicates an example of experimental results by the conventional state feedback control, where the specimen on table includes the resonant/anti-resonant characteristics in the frequency of around 6.6 Hz. From the figure, effects of the resonance in specimen obviously deteriorates the performance accuracy in the power spectrum. For the performance deterioration, several attempts, such as an adaptive control and/or a MCS(Stoten and Gomez, 1998), and a real-time compensation(Dozono *et al.*, 2004), have been adopted to compensate for the effects of resonance in specimen. Those approaches, however,

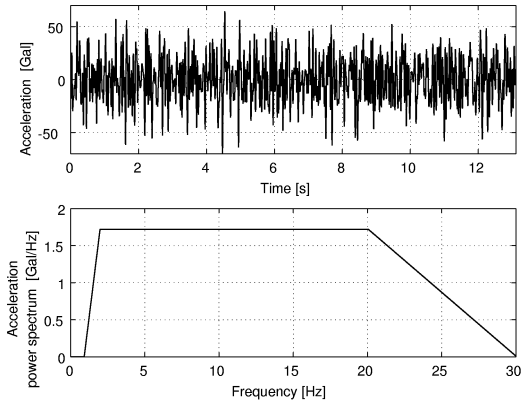

Fig. 4. Waveform and frequency power spectrum in desired acceleration reference.

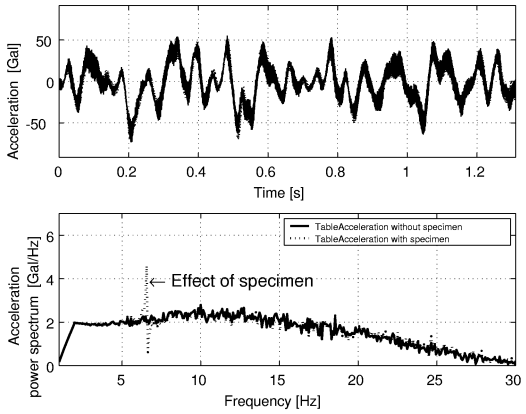

Fig. 5. Experimental results of time response and power spectrum in acceleration by conventional control. (specimen with resonant frequency of 6.6 Hz)

are insufficient, due to the limitation of adaptation capability in speed, for the nonlinear behaviors in specimen, e.g., the variation of resonant characteristics during the damage process and the nonlinear components.

3. COMPENSATION FOR REACTION FORCE USING DISTURBANCE OBSERVER

3.1 Configuration of disturbance observer

Performance improvements in the frequency power spectrum using a disturbance observer(Ohnishi *et al.*, 1996) are attempted in the proposed control, where the effects of resonance in specimen on the power spectrum are compensated as the reaction force suppression. In the target system, the disturbance observer is constructed using the measured state variables, allowing the performance deterioration due to modeling errors to be improved.

Eqs.(1)-(5) can be synthesized and simplified as follows, using the definition of parameters/variables listed in Table 3:

Table 3. Definition of parameters and variables in plant system.

g_{sv}	$\frac{s^2+2\zeta W_{sv}s+W_{sv}^2}{K_{sv}W_{sv}^2}$	g_{pr}	$K_{pr}F_{pr}$
g_k	$K_a s + C_{al}$	g_a	A_a
g_{pm}	$M_a s^2 + C_{al} s$	g_{tm}	$M_t s^2$
g_c	$C_j s + K_j$		

$$\frac{1}{g_{sv}}(E-U) = (g_k + \frac{g_{pr}}{g_{sv}})P_m + g_a\, sY_p, \quad (11)$$

$$(g_{pm}+g_c)Y_p = g_a P_m + \frac{g_c Y_{ta}}{s^2}, \quad (12)$$

$$\frac{(g_{tm}+g_c)g_c Y_{ta}}{s^2} = g_c Y_p - D, \quad (13)$$

where U is an equivalent displacement disturbance for the reaction force of specimen, which should be compensated for.

Eqs.(11)-(13) lead to the following, concerning the displacement feedback compensation signal E:

$$E = U + G_D D + G_Y Y_{ta}, \quad (14)$$

$$G_D = \frac{(g_{sv}g_k + g_{pr})(g_{pm}+g_c) + g_{sv}g_a^2 s}{g_a g_c},$$

$$G_Y = \frac{(g_{sv}g_k + g_{pr})(g_{tm}g_{pm} + g_c g_{tm} + g_{pm}g_c)}{g_a g_c s^2} + \frac{(g_{tm}+g_c)g_{sv}g_a^2 s}{g_a g_c s^2}.$$

From eq.(14), a desired value U, which compensates for the effect of disturbance D, can be given as:

$$U = -G_D D. \quad (15)$$

Since the disturbance in eq.(15) is unobservable, it should be estimated by the mathematical model in eqs.(11)-(13).

3.2 Design of disturbance observer

A disturbance estimation $\widehat{D}$ can be performed by combining eqs.(12) and (13), using the measured state variables: the differential pressure in cylinder P_m and the table acceleration Y_{ta}:

$$\widehat{D} = \frac{g_a g_c}{g_{pm}+g_c}P_m - \frac{g_{tm}+g_c}{s^2}Y_{ta}. \quad (16)$$

By considering the practical estimation, eq.(16) can be simplified as follows, since effects of the hydrostatic coupling on the estimation should be negligible.

$$\widehat{D} = g_a P_m - \frac{g_{pm}+g_{tm}}{s^2}Y_{ta} \quad (17)$$

The equivalent displacement disturbance, as a result, can be compensated by the following principle, by combining G_D in eq.(14) and U in eq.(15):

$$U = -\frac{g_{sv}g_k + g_{pr}}{g_a}\widehat{D}. \quad (18)$$

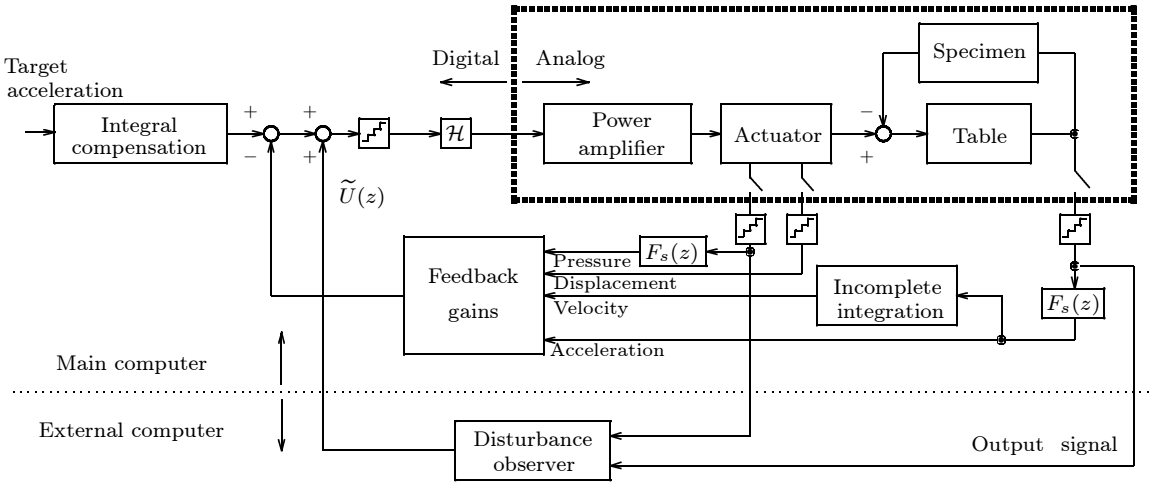

Fig. 6. Actual block diagram of control system with disturbance observer.

Since the synthesized disturbance estimator is composed of the measured state variables, the effects of the mathematical modeling errors on the estimation can be simultaneously included as equivalent disturbances in eq.(17), allowing the deterioration of disturbance suppression due to the modeling errors to be improved.

Structural configuration of the disturbance estimator in eq.(17), on the other hand, is un-proper, which prevents the compensation from being practically implemented. In addition, the measured table acceleration signal contains a sensor drift and/or noise components. The actual implementation, therefore, can be performed as a disturbance observer $\widetilde{U}$, by adding the following two filters: G_L making the observer to be proper and G_B for the sensor noise/drift.

$$\widetilde{U} = G_L G_B \widehat{U} \tag{19}$$

$$G_L = \left(\frac{\omega_l}{s + \omega_l} \right)^3$$

$$G_B = \left(\frac{\omega_b s}{s^2 + (\omega_a + \omega_b)s + \omega_a \omega_b} \right)^6$$

The natural frequency in the observer filter G_L is selected as $\omega_l = 2\pi \times 250$ Hz, providing the frequency bandwidth up to 20 Hz in the seismic motion performance. The band-pass filter G_B for the acceleration sensor drift/noise compensation, on the other hand, is composed of a 12th-order filter with the natural frequencies of $\omega_a = 2\pi \times 0.5$ Hz and $\omega_b = 2\pi \times 500$ Hz, respectively.

4. EXPERIMENTAL VERIFICATIONS

The proposed control with the disturbance observer-based compensation for the reaction force in specimen has been verified by a series of experiments. The whole control processing is performed by multi-Digital Signal Processors (DSPs), where the feedback/feedforward compensators and the disturbance observer are processed by the respective DSPs as shown in a block diagram of Fig.6. The same target acceleration signal as of Fig.4 is given

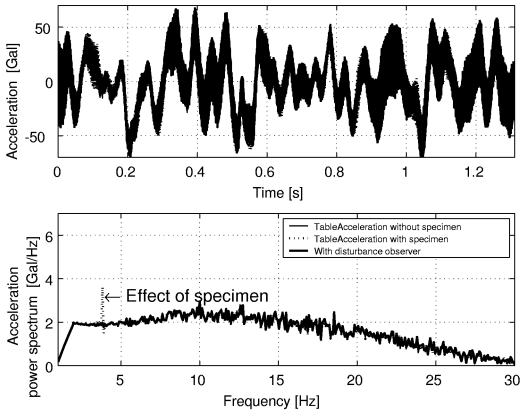

Fig. 7. Experimental results of time response and power spectrum in acceleration by proposed control. (specimen with resonant frequency of 3.9 Hz)

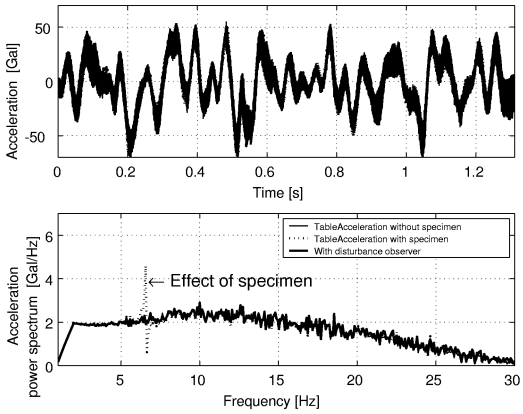

Fig. 8. Experimental results of time response and power spectrum in acceleration by proposed control. (specimen with resonant frequency of 6.6 Hz)

to evaluate the reproducibility of the frequency power spectrum.

Figs.7 and 8 show the experimental results of time response and power spectrum in acceleration by the proposed compensation, in the cases that the specimen includes the resonance frequency of 3.9 or 6.6 Hz, where the variation in resonance frequency simulates the nonlinear behavior of the specimen. In the figures, the proposed compensation depicted in solid lines can exactly reproduce the power spectrum as of the one without specimen, while dotted lines without compensation are deteriorated by effects of the reaction force in specimen.

5. CONCLUSIONS

In the paper, a novel control strategy of the shaking table for seismic tests is proposed, where the disturbance observer effectively compensates for the effects of reaction force in target specimen on the reproducibility of the desired table acceleration. The nonlinear behavior in the specimen can be simultaneously compensated for, and as a result, the precise table motion control can be obtained under the arbitrary specimen with the variation of resonant frequency during the seismic test.

REFERENCES

Clark, A.J. (1992). Dynamic characteristics of large multiple degree of freedom shaking tables. *Proceedings of 10th World Conference on Earthquake Engineering* pp. 2823–2828.

Dozono, Y., T. Horiuchi, H. Katsumata and T. Konnno (2004). Shaking-table control by real-time compensation of the reaction force caused by a nonlinear structure. *Transactions of the ASME, Journal of Pressure Vessel Technology* **126-2**, 122–127.

Gomez, E.G. and D.P. Stoten (2000). A comparative study of the adaptive MCS control algorithm on European shaking-tables. *Proceedings of 12th World Conference on Earthquake Engineering* **2626**, 1–8.

Nowak, R.F., D.A. Kunsner, R.L. Larson and B.K. Thoen (2000). Utilizing modern digital signal processing for improvement of large scale shaking table performance. *Proceedings of 12th World Conference on Earthquake Engineering* **2035**, 1–8.

Ohnishi, K., M. Shibata and T. Murakami (1996). Motion control for advanced mechatronics. *IEEE/ASME Transactions on Mechatronics* **1-1**, 56–67.

Okuda, Y., A. Maekawa, C. Yasuda and M. Sakuno (2001). Development of the control method of shaking table for collapse test. *Proceedings of the 2001 ASME Pressure Vessels and Piping Conference* **428-1**, 227–231.

Queval, J.C. and P. Sollogoub (1997). Large scale seismic tests performed on the table Azalee of CEA -Reproducibility of seismic motions. *Transactions of the 14th International Conference on Structural Mechanics in Reactor Technology* pp. 237–245.

Stoten, D.P. and E.G. Gomez (1998). Recent application: Results of adaptive control on multi-axis shaking tables. *Seismic Design Practice into the Next Century* pp. 381–387.